*Plasma Medicine*, 6(1):85–100 (2016)

# $He/H_2$ Pulsed-Discharge Plasma as a Tool for Synthesis of Surfactant-Free Colloidal Silver Nanoparticles in Water

Aleksei Treshchalov,* Sergey Tsarenko, Tea Avarmaa, Rando Saar, Ants Lõhmus, Alexander Vanetsev, & Ilmo Sildos

Institute of Physics, University of Tartu, Tartu, Estonia

*Address all correspondence to: Aleksei Treshchalov, Institute of Physics, University of Tartu, 14c Ravila Street, 50411 Tartu, Estonia, E-mail: atr@ut.ee

**ABSTRACT:** In this study we investigated the interaction of atmospheric-pressure helium (He) and He/$H_2$ pulsed-discharge plasma with different water solutions. We developed a synthetic path to obtain fairly uniform, small (~2 nm), surfactant-free silver (Ag) nanoparticles (NPs) with the treatment of an $AgNO_3$ solution with He/$H_2$ bipolar pulsed discharge. The colloidal solutions containing Ag NPs are stable for months and do not show any agglomeration (the measured zeta potential is −41 mV at pH ~8). The adsorption of negatively charged hydroxide ($OH^-$) ions on the surface of Ag NPs could be responsible for the electrostatic stabilization. The treatment of the air-saturated water by pure He plasma with a negative polarity leads to the creation of $HNO_3$ and hydrogen peroxide ($H_2O_2$) as stable species. Contrary to the acidification of the solution by He plasma treatment, He/$H_2$ discharge with negative and, in particular, with bipolar pulses produces only traces of $HNO_3$ and no $H_2O_2$. We demonstrate here that He/$H_2$ discharge with bipolar pulses is remarkably efficient in near-complete nitrate decomposition and slight alkalization of dilute $HNO_3$ and $KNO_3$ solutions.

**KEY WORDS:** alkalization, bipolar discharge, denitrification, electrostatic stabilization, helium, hydrogen, nanoparticle, plasma, plasma–liquid interface, silver

## I. INTRODUCTION

Metal nanoparticles (NPs) have many promising applications: as components of electric devices, catalysts, antibacterial agents, fluorescent labels, and in biochemical sensing, among others. However, the synthesis of pure, homogeneous, and stable NPs remains a challenging task for nanotechnology. The surface of noble metal NPs synthesized by traditional "wet" chemical reduction methods is usually contaminated by reducing agent residues, surfactants, and stabilizers. These impurities cannot be easily removed from the surface of NPs without affecting their physical and chemical properties. This problem could partially be solved by using radiolysis techniques, where chemically active radicals are formed as a result of ionization and excitation of the solvent molecules by electrons, α particles, or photons of X- and γ-radiation.[1] Direct reduction of metal ions in water with hydrated electrons ($e_{aq}$) seems to be the cleanest approach to obtain NPs with clean surface.[2] Other than the desirable reducing species ($e_{aq}$, ·H), however, particles with strong oxidizing properties (·OH, hydrogen peroxide [$H_2O_2$]) are inevitably formed as a result of the high energy involved.[1] Specific scavengers like alcohols are used to eliminate oxidizers. Moreover, soluble polymers are added to stabilize metal

2151-805X/16/$35.00  

NPs, preventing spontaneous agglomeration of the NPs.[3] Pulsed laser ablation of a metal substrate in liquids seems to be another promising technique that is capable of providing totally ligand-free NPs,[4] but its low efficiency and poor control over the shape and size distribution of the particles are disadvantages of this method.

The plasma treatment of aqueous solutions forms the basis of various promising new technologies for water purification, nonequilibrium chemical processing of nanomaterials, and plasma medicine. Synthesis of metal NPs by means of electrochemical processes occurring during a plasma–liquid interaction is currently a quickly developing and cost-effective technique.[5–9] This method produces chemically active radicals from the gas or solution molecules at the plasma–liquid interface. The resulting electrochemical processes can be controlled in 2 ways, either (1) in the solution phase, as in usual "wet" chemical reduction methods, by varying the chemical composition of the reaction mixture and the concentrations of reagents, or (2) in the plasma phase by adjusting the energy and composition of plasma species. This provides us with flexibility to tune the chemical nature and concentrations of different reducing or oxidizing species in the solution. The main advantages of this technique are its relative simplicity, the minimum number of additional chemical reagents, the high reaction yield, the fast processing rates at room temperature, and the (usual) absence of side products. Most important, it is possible to avoid surfactants because the synthesized NPs usually are stabilized electrostatically. The plasma-assisted electrochemical process has already been successfully used to synthesize silver (Ag) NPs.[6,10] Without stabilizing additives, however, a narrow range of Ag NP sizes is difficult to obtain.

The aim of this work was to study the interaction of an atmospheric-pressure helium(He) and helium/hydrogen (He/H2) pulsed-discharge plasma with different aqueous systems. The results were used to develop a new approach to the synthesis of small, surfactant-free Ag NPs that are stable in a colloidal solution. The principal task was to elucidate the pathways of Ag NP formation and the nature of their electrostatic stabilization. Efficient nitrate ion ($NO_3^-$) decomposition in diluted $HNO_3$ and $KNO_3$ solutions and their alkalization by plasma treatment were also demonstrated and are discussed here.

## II. MATERIALS AND METHODS

The reaction vessel for plasma treatment of different water solutions is shown in Figure 1. Experiments were performed in a closed silica cell under continuous gas flow, typically 150 $cm^3$ $min^{-1}$ (sccm). The pulsed-discharge plasma was initiated at the atmospheric pressure in a He or mixed He + 5% $H_2$ gas jet between a stainless steel capillary tube (with a 0.3-mm inner diameter) and an aqueous electrolyte with an immersed, grounded platinum (Pt) wire electrode. The capillary tube was placed 20 mm from the Pt wire, and a discharge gap of about 6 mm was left between the liquid surface and the gas outlet. Intense stirring of the solution carries the products of the plasma–liquid interaction away from the plasma spot (~2 mm in diameter) on the liquid surface. He and $H_2$ gases with a purity of 6.0 and 5.0, respectively, were used in the experiments.

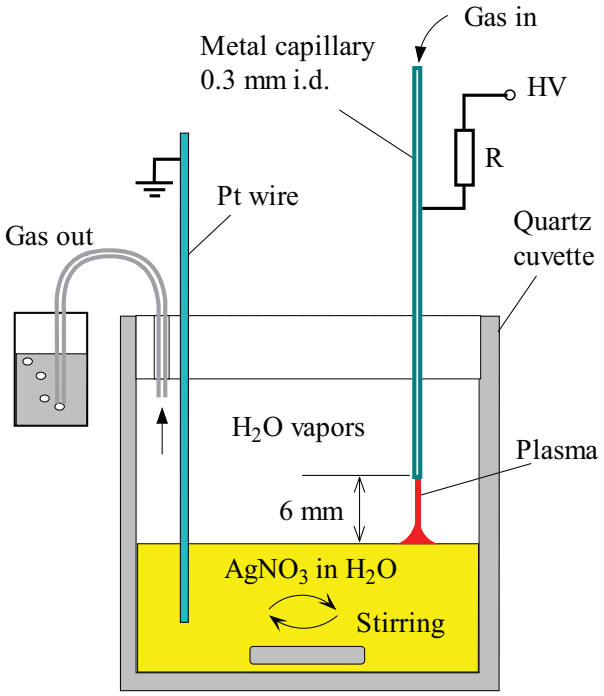


**FIG. 1:** The scheme of the experimental setup. HV, high voltage; i.d., inner diameter; Pt, platinum; R, resistor for the current measurement.

Pulsed discharge has several advantages over a direct current regime; in particular, it is more stable against the glow-to-arc transition. Pulsed excitation allows one to apply a higher peak power, while keeping the average power low to avoid overheating the solution. As an additional benefit, monitoring of the kinetics of plasma chemical reactions becomes possible. The bulk temperature of liquid did not exceed 50°C during the plasma processing. The plasma jet appears very homogeneous upon visual inspection. A homemade pulsed generator was used for plasma excitation. It produces bipolar (alternating) pulses (up to 10 kV) with a repetition rate of 12 kHz. Rectifier diodes select the pulse voltage polarity of the generator's output. Thus the capillary can operate as either a negative (cathode) or positive (anode) electrode with respect to the liquid surface. In this work we used discharges with negative and bipolar excitation pulses. The treatment of electrolytes by discharge with a positive polarity on the capillary was avoided because of the electrolytic cathodic processes (e.g., the deposition of Ag) on the Pt electrode.

The electrical characteristics of discharge were recorded with a TDS 3054B 500 MHz oscilloscope and a P6015 high-voltage probe (both Tektronix Inc., Beaverton, OR). The voltage and current waveforms were determined on a resistor R connected to a high-voltage electrode.

The absorption spectra of solutions were recorded on a Jasco V-570 ultraviolet (UV)/visible/near-infrared spectrophotometer. Stable chemical species ($H_2O_2$, $NO_3^-$,

and hydroxide [$OH^-$] ions) present in water or produced after the plasma treatment were detected by their characteristic UV absorption bands. The background spectrum from a 1-cm silica cell filled with deionized water was subtracted from all measured spectra so the spectral features with small absorbance could be more clearly observed and analyzed. The initial solutions of $AgNO_3$ (1 mmol/L), $KNO_3$ (1 mmol/L), $HNO_3$ (1 mmol/L), KOH (1 mmol/L), and $H_2O_2$ (10 mmol/L) were prepared using analytical-grade reagents and deionized Milli-Q water. For each experiment, solutions were diluted with deionized Milli-Q water to achieve the desired concentrations. One should keep in mind that, according to Henry's law, the equilibrium concentrations of air gases in water at ambient conditions are $O_2$, 0.26 mmol/L; $N_2$, 0.4 mmol/L; $CO_2$, 0.014 mmol/L.[11] Thus, the water used was slightly acidic (pH 5.6) because of the dissolved $CO_2$.

A Metrohm 930 Compact IC Flex ion liquid chromatograph was used to analyze the cation concentration in the solution after the plasma treatment. The hydrodynamic diameter and the surface charge (characterized by zeta potential) of Ag NPs in the solution were measured with a Zetasizer Nano ZSP system (Malvern Instruments) using dynamic light scattering (DLS) and electrophoretic light scattering techniques, respectively. The size distribution of Ag NPs was also estimated by scanning electron microscopy (SEM) images taken using a Helios Nanolab 600 device (FEI, Hillsboro, OR) operated at 10 kV. The SEM probes were prepared by depositing a drop of the solution on a silicon substrate that was left to dry in air. The plasmonic band position and width in the UV/visible extinction spectra were also used to assess the Ag NPs size distribution. A portable pH meter (pH-98103R; Analytical Instruments) was used to measure the pH of solutions.

## III. RESULTS AND DISCUSSION

### A. Electrical Characteristics of the Discharge

The power supply produces a perfect sinusoidal waveform of voltage in the absence of breakdown at the discharge gap. In the regime of the gas breakdown, however, the shape of pulses becomes almost rectangular, as the output current is limited by the internal resistance of the generator. This resistance is much higher than the resistance of the plasma and electrolyte (the resistance of an 0.1 mmol/L $AgNO_3$ aqueous solution is about 20 kΩ). Figure 2 shows waveforms of basic electrical characteristics for He + 5% $H_2$ discharge with bipolar excitation. The shunt resistor R (18 kΩ) was used to measure the current. At a negative polarity on the capillary, when the cathode layer is formed at the hot and sharp tip of the metal capillary, the breakdown voltage is lower than that which occurs with a positive polarity, when the cathode layer is the flat surface of a cold electrolyte. As a consequence, the amplitude of a negative current pulse is less and its duration is longer than those of a positive pulse, but the integral current is very close to zero. Oxygen ($O_2$) or $H_2$ gas bubbles did not appear to evolve near the Pt electrode in this bipolar pulsed-current regime. However, short-lived active species ($\cdot O$, $\cdot H$, $e_{aq}$) are generated in the plasma–liquid interface, just as in the case of a fixed polarity. Plasma treatment of water solutions by bipolar pulse excitation of a $He/H_2$ gas mixture seemed

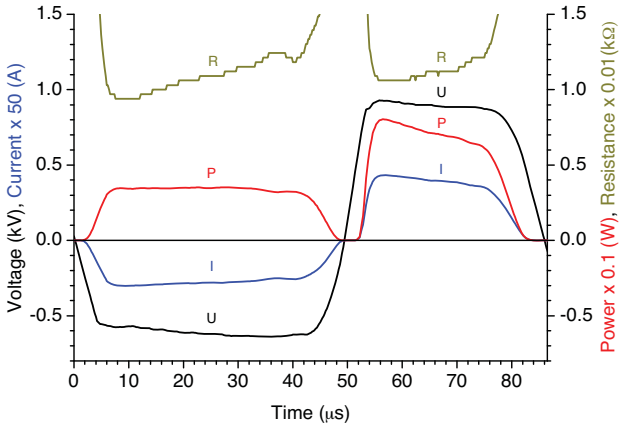


**FIG. 2:** Time dependence of basic discharge parameters (bipolar excitation) for an He + 5% $H_2$ jet with a flow of 150 sccm. U, the voltage drop on the discharge plasma and the electrolyte (0.1 mmol/L $AgNO_3$); I, the discharge current; R, the resistance (plasma with electrolyte); P, the discharge power, calculated by multiplying the current and voltage waveforms.

to be the most efficient for nitrate decomposition (denitrification) and alkalization of the solution. Such discharge is also more favorable for the synthesis of small Ag NPs with a narrow size distribution.

## B. Absorption Spectra of Plasma-Treated Aqueous Solutions: Diagnostics of Stable Species in the Liquid Phase

During the plasma jet treatment of a solution, a net transfer of charge from the plasma into the liquid takes place in the form of ions and electrons. Moreover, reactive species (excited atoms and radicals) are produced not only in the laminar flow of the jet core but also in the boundary region where core gases diffuse and mix turbulently with water vapors. The plasma–liquid interface is of a special interest because a high-humidity region forms near the electrolyte surface; this is due to the conical expansion of a jet along the surface, where the direction of the gas flow changes from vertical to horizontal.[12] The formation mechanisms of active species in the plasma and at the plasma–water interface were elucidated in our experiments with the aid of spatial, time-resolved emission spectroscopy of the discharge. These diagnostic data will be published separately in full detail. In this article we intentionally focus only on the stable molecular and ionic compounds that accumulated in the liquid phase as a result of the rapid solvation and transformation of short-lived plasma species passing through the water surface.

In several important applications of the plasma processing of aqueous systems, such as water purification, decontamination, and plasma medicine, maximum production of oxidizing species such as ·OH, ·O, $H_2O_2$, and $H^+$ is necessary. As an example, the treatment of water by plasma containing air leads to acidification (resulting from the dissolution of $NO_x$ species generated in the plasma) and the creation of $H_2O_2$ in a 3-body

recombination reaction of hydroxyl radicals in water ($\cdot OH_{aq} + \cdot OH_{aq} \rightarrow H_2O_{2aq}$).[13,14] However, the reducing properties of plasma are required in certain applications, for example, reducing species ($e_{aq}$, $\cdot H$) must participate in the synthesis of metal NPs. The presence of oxidizing species could be harmful in these processes owing to the oxidative etching of metal NPs; they can, however, play also a positive role in the controlled synthesis of metal nanocrystals.[15]

In our experiments the properties of solutions following the plasma treatment strongly depended on the gas composition of the plasma and the polarity of the discharge. To more closely study these phenomena, absorption spectra of several model solutions were recorded before and after processing with He and He/$H_2$ plasmas. Figure 3 displays reference UV absorption spectra for several common ions and molecules in water. As expected, the salts and the strong acids and bases are fully dissociated, so that the absorption bands belong to hydrated ions. For example, the spectra of 0.1-mmol/L solutions of $AgNO_3$, $KNO_3$, and $HNO_3$ are nearly identical and assigned to anion $NO_3^-$. It follows from Fig. 3 that the stable species, which could be produced in water during the plasma treatment, have characteristic absorption bands. The following curve-fitting procedure was used for the quantitative analysis of the solutions after treatment.

To distinguish inputs to the absorption of $H_2O_2$ and $NO_3^-$ ($OH^-$), we used the difference in absorption at various spectral regions. The concentration of $H_2O_2$ was determined using the value of absorption in the range of 250–260 nm, where $NO_3^-$ ($OH^-$) species have zero absorption. The deep UV region (200–240 nm) was modeled as the sum of the absorption of $H_2O_2$ and $NO_3^-$ ($OH^-$) species. The applicability of the curve-fitting procedure was confirmed by additional reference experiments. The absorbance of the series of solutions with known concentrations of $HNO_3$ (up to 0.2 mmol/L), $H_2O_2$ (up to 7.25 mmol/L), and their mixtures were measured. No interference between signals of $NO_3^-$ and $H_2O_2$ was observed. The absorbance signal of the mixed solution of $HNO_3$ and

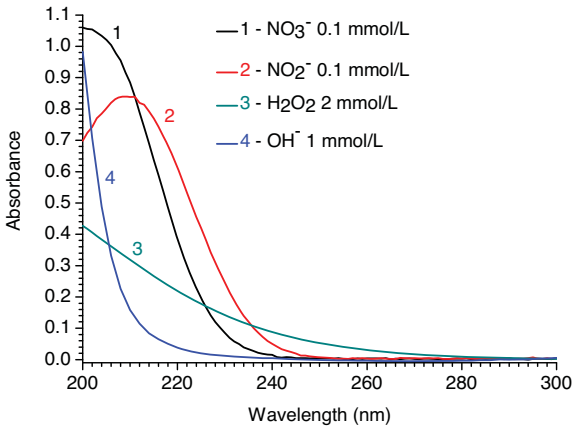


**FIG. 3:** Ultraviolet absorption spectra for stable species in different water solutions: (1) $NO_3^-$ anions in 0.1 mmol/L $AgNO_3$; (2) $NO_2^-$ anions in 0.1 mmol/L $KNO_2$; (3) hydrogen peroxide ($H_2O_2$) molecules in 1 mmol/L $H_2O_2$; (4) $OH^-$ anions in 1 mmol/L KOH.

$H_2O_2$ was the same as the calculated sum of the absorbances of the individual components. The estimated inaccuracy of the fitting was around 2% (this was dependent on the signal-to-noise ratio of the absorption curve).

Figure 4 shows the absorption spectra and pH parameter of deionized water after treatment by the He and He + 5% $H_2$ plasma jet, with different polarities at the capillary electrode. It follows from curves 1 and 5 in Figure 4 that during 5 minutes of plasma treatment (He discharge with a negative polarity), $HNO_3$ (0.04 mmol/L) and $H_2O_2$ (1.1 mmol/L) are produced. The corresponding shift to an acidic pH (4.4) of the solution was detected. Deaeration of water by bubbling with an He flow of 150 sccm for 15 min before the plasma processing decreased the concentration of $HNO_3$ by a factor of 4. As expected, treatment with an He plasma jet containing traces of air results in the formation of more $HNO_3$, with the concentration reaching 0.2 mmol/L (pH 3.7). The absorption in the region of characteristic bands of nitrite ($NO_2^-$) ions and dissolved $O_3$ molecules at 256 nm, and peroxynitrite ions at 302 nm, was below detection limits in our solutions after treatment.[15,16] These results are similar to those obtained in Ref. 17.

Contrary to the He plasma treatment, the He/$H_2$ discharge with negative or, especially, bipolar pulses produces only traces of $HNO_3$ (0.01 mmol/L) and no $H_2O_2$ (see curves 2 and 6 in Fig. 4). The deaeration of water before He/$H_2$ plasma processing helps to suppress the formation of $HNO_3$ even more (see curves 3 and 4 in Fig. 4).

The different results of He and He/$H_2$ plasma treatments can be explained as follows. In the He discharge, the $He_2^+$ ions and He metastable atoms effectively ionize water and

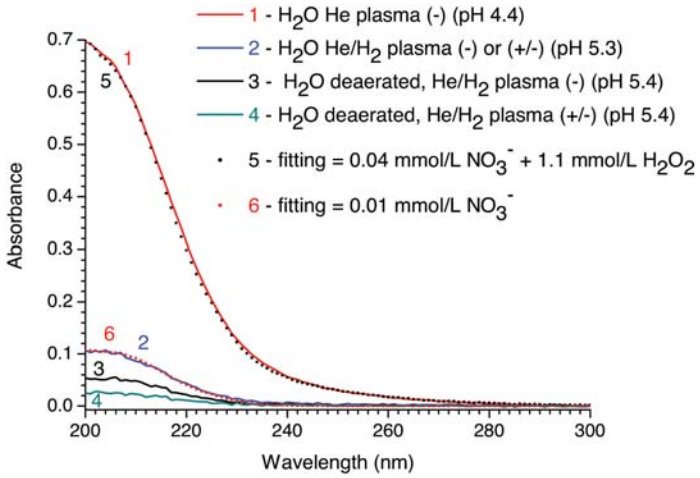


**FIG. 4:** Absorption spectra of water after the treatment with plasma with different polarities. (1) 5 minutes of helium (He) plasma (negative [−] polarity); (2) 5 minutes of He/$H_2$ plasma, negative or positive (+)/negative pulse; (3) 5-minute treatment of deaerated water by He/$H_2$ plasma (negative polarity); (4) 5-minute treatment of deaerated water by He/$H_2$ plasma (bipolar pulse); (5) fitting of curve 1 by the sum $NO_3^-$ (0.04 mmol/L) + hydrogen peroxide ($H_2O_2$; 1.1 mmol/L); (6) fitting of curve 2 by $NO_3^-$ (0.01 mmol/L).

produce the $H_2O^+$ ions, which quickly react with water to produce hydroxonium ($H_3O^+_{aq}$; determining the pH) and hydroxyl radicals ($\cdot OH_{aq}$).[14] The $\cdot OH_{aq}$ radicals are the main precursors of $H_2O_2$. The $NO_3^-$ negative ions (which conjugate to $H_3O^+_{aq}$ ions) are formed from $O_2$ and nitrogen ($N_2$) molecules dissolved in water or in the gas above the liquid. In the presence of air, the He discharge produces $NO_x$ radicals that can form $NO_3^-$ and increase the acidity of the solution.

In the case of $He/H_2$ plasma, the concentration of highly energetic He metastable atoms and He-containing ions at the plasma–water interface decreases significantly as a result of the lower electron temperature in the discharge. As a result, the degree of ionization and dissociation of $H_2O$ decreases, since the recombination flow is coming mainly through $H_2^+$ ions. Thus $He/H_2$ plasma produces no $H_2O_2$ and only traces of $HNO_3$.

The capability of $He/H_2$ plasma with an alternating polarity to decompose $NO_3^-$ ions in diluted nitric acid solutions can be remarkably effective (see Fig. 5). Curve 1 shows the absorption of the initial solution of 0.1 mmol/L $HNO_3$ (pH 4). After 10 minutes of treatment by an $He/H_2$ discharge with bipolar pulses, 90% of the $NO_3^-$ ions disappear, whereas 20 minutes of plasma treatment decomposes about 99% of $NO_3^-$ ions. No production of $H_2O_2$ was observed, and a shift to basic pH values occurred (pH 8.9). The presence of $NH_4^+$ cations (as the conjugate to $OH^-$ anions) was confirmed by liquid ion chromatography, which detected about 0.03 mmol/L of $NH_4^+$ in the solution after treatment. Consequently, $He/H_2$ plasma treatment can transform an acid to a base. Similarly, almost complete decomposition of $NO_3^-$ ions and an even stronger shift to basic pH values were observed in 0.1 mmol/L $KNO_3$ (see Fig. 6). Curve 1 shows the absorption of the initial solution of 0.1 mmol/L $KNO_3$ (pH 5.6). After 10 minutes of

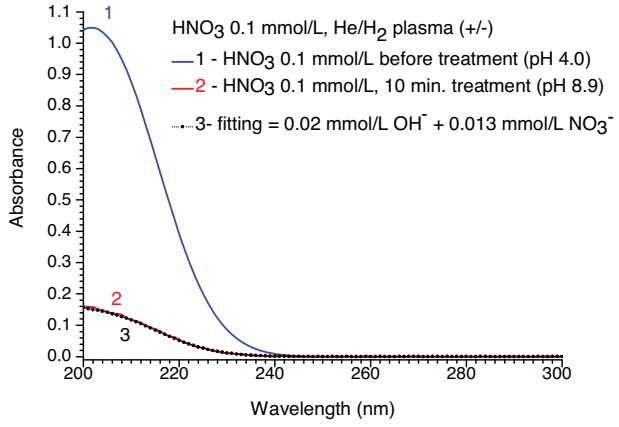


**FIG. 5:** Absorption spectra of water solution (0.1mmol/L $HNO_3$) before and after treatment with helium (He) + 5% $H_2$ plasma with bipolar pulsed excitation. (1) before plasma treatment (pH 4.0); (2) 10 minutes of $He/H_2$ plasma treatment (pH 8.9); (3) fitting of curve 2 by the sum $OH^-$ (0.02 mmol/L) + $NO_3^-$ (0.013 mmol/L). $He/H_2$ plasma treatment transforms the acid into a base.

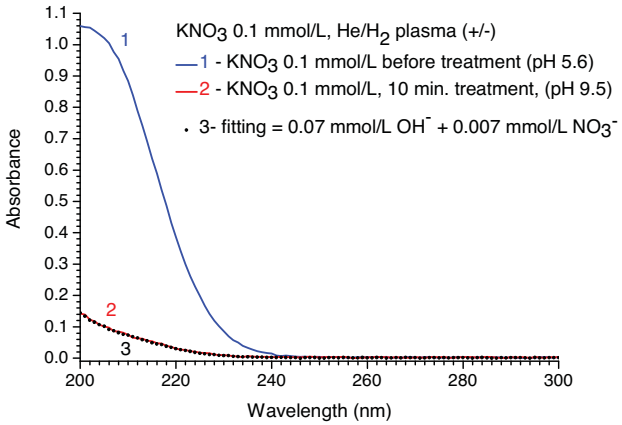


**FIG. 6:** Absorption spectra of water solution (0.1mmol/L $KNO_3$) before and after treatment with helium (He) + 5% $H_2$ plasma with bipolar pulsed excitation. (1) before plasma treatment (pH 5.6); (2) 10 minutes of He/$H_2$ plasma treatment (pH 9.5); (3) fitting of curve 2 by the sum $OH^-$ (0.07 mmol/L) + $NO_3^-$ (0.007 mmol/L).

treatment by the He/$H_2$ discharge with bipolar pulses, more than 90% of $NO_3^-$ ions disappeared. No production of $H_2O_2$ was observed, and a shift to a basic pH value occurred (pH 9.5).

In contrast to the treatment by an He/$H_2$ discharge with bipolar pulses, using either a negative or positive polarity decomposes only about 10% of $NO_3^-$ ions in the 0.1 mmol/L $HNO_3$ solution, with the pH changing only slightly from 4.0 to 4.5. The influence of alternating polarity in the neat He plasma was studied, and again, after the treatment of 0.1 mmol/L $HNO_3$ with bipolar pulses, pH increased only slightly to 4.5. These results allow the direct electrochemical reduction of $NO_3^-$ ions on the surface of Pt electrode (despite its catalytic activity) to be excluded from consideration as the possible mechanism of decomposition of $NO_3^-$ ions.

It can be concluded that chemical reactions at the plasma–liquid interface, with participation of hydrated electrons and ·H radicals in dilute $HNO_3$ and $KNO_3$ solutions, cause nearly complete decomposition of $NO_3^-$ ions and a shift to basic pH values. A total $NO_3^-$ reduction can formally involve 8 single-electron transfer steps in a sequence, accompanied by the attachment of protons: $NO_3^- \rightarrow NO_2^- \rightarrow N_2O_3 \rightarrow NO \rightarrow N_2O \rightarrow N_2 \rightarrow NH \rightarrow N_2H_4 \rightarrow NH_3$. Obviously, not all $NO_3^-$ is transformed to $NH_4^+$ because the gaseous products (NO, $N_2$, $N_2O$) can escape the solution. Hydrated electrons and ·H radicals are very short-lived species, and therefore the reduction reactions can take place only within a radius of several nanometers.[19] When specific scavengers are absent, the hydrated electrons are quickly subjected to a second-order recombination and form $OH^-$ and hydrogen: $2H_2O + 2e_{aq} \rightarrow 2OH^-_{aq} + H_2$, with a rate constant of $2k = 1.1 \times 10^{10}$ $M^{-1}$ $s^{-1}$.[20] The local increase in pH within the plasma–liquid surface layer can be significant because of this electrolysis reaction.[21,22]

The surprising difference in the efficiency of decomposition of $NO_3^-$ ions between bipolar (~90%) and negative-polarity (~10%) plasma processing can be explained by the migration of $NO_3^-$ ions in the surface electric field. During the treatment with the discharge with bipolar pulses, the $NO_3^-$ ions move back and forth in the interface layer (in a vertical direction), whereas at a negative polarity the interface is depleted of $NO_3^-$. Despite intense stirring, the liquid on the surface moves only at a speed of about 10 mm/second in a horizontal direction through the plasma spot (~2-mm diameter), so that during the 12-kHz discharge the local volume at the interface is subject to about 2400 pulses before leaving the reaction zone.

## C. Synthesis of Surfactant-Free Ag NPs in an $AgNO_3$ Solution by Plasma-Induced Reduction

Reducing agents obtained by cathode plasma treatment of water solutions could be used for the preparation of metal NPs. This section focuses on the substantial differences between the He and $He/H_2$ plasma treatments of $AgNO_3$ aqueous solutions with regard to the efficiency of Ag NP production, their size distribution, and electrostatic stabilization. Figure 7 shows the absorbance of a 0.1-mmol/L $AgNO_3$ solution before (curve 1) and after (curve 2) the He plasma treatment with negative-pulsed voltage for 60 seconds. A slight decrease of the pH—from 5.6 to 4.5—was noticed. The nature of this effect could be similar to that discussed earlier for pure water (Fig. 4). Plasma produces extra nitric acid in a coupled reaction oxidizing $N_2$ into $NO_3^-$ and electron detachment from water (by $He_2^+$ ions and He metastable atoms), releasing protons in the form of $H_3O^+$ ions. In addition, the hydrated electrons reduce $Ag^+$ cations to the neutral state $Ag^0$. As pH decreases, the concentration of $Ag^+$ cations decreases too, and the concentration of $H_3O^+$

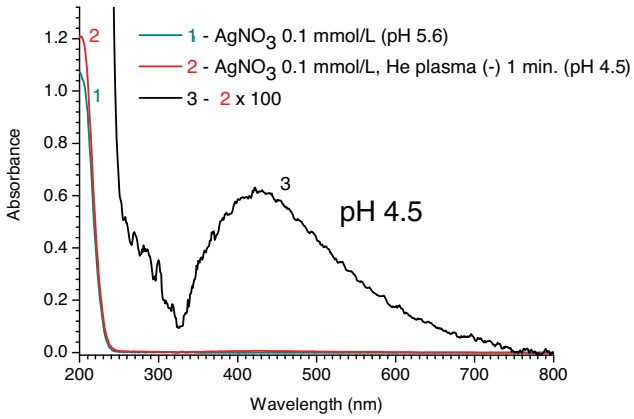


**FIG. 7:** Absorption spectra of water solution (0.1 mmol/L $AgNO_3$) before (1) and after (2) 1 minute of helium plasma treatment with a negative polarity. Curve 3 is curve 2 multiplied by 100. The weak and broad band peaking at 420 nm presumably belongs to small (~1 nm), stable $Ag_n$ clusters.

ions increases, while $NO_3^-$ counter-anions serve as a conjugate agent to preserve charge neutrality. One should keep in mind that $H_2O_2$ is also produced during the He plasma treatment (Fig. 4).

The liquid remains transparent, though a weak and broad absorption band with a maximum at 420 nm appears (curve 3 in Fig. 7). This band can presumably be assigned to the plasmonic absorption of very small (~1 nm) $Ag_n$ clusters. According to earlier reports, with a diminishing diameter of $Ag_n$ clusters, the intensity of the plasmonic absorption decreases and the band is redshifted and strongly broadened.[23,24]

It is also known that in acidic conditions the oxidative etching of Ag NPs by $H_2O_2$ takes place.[18] It is rather surprising that Ag NPs can still exist in this environment. The surviving clusters could later serve as seeds for the growth of larger Ag NPs. An attempt to detect these clusters in the SEM probes prepared on a silicon substrate was not successful because of the insufficient resolution of the SEM technique.

To minimize acidification and avoid the formation of $H_2O_2$, treatment with He + 5% $H_2$ discharge with bipolar pulses was used. Figure 8 shows an SEM image of Ag NPs obtained after 5 minutes of plasma processing of 0.1 mmol/L $AgNO_3$ in this regime. Two sorts of Ag NPs can be seen in this micrograph: the relatively large (15–25 nm), loose agglomerates stand out against the background of a large number of tiny NPs (~3 nm), whose sizes and shapes are difficult to measure because of insufficient resolution. Because of the relatively small sampling area in SEM probes, the statistical size distribution depicted in Fig. 8 may not fully represent the liquid sample. Preparation of

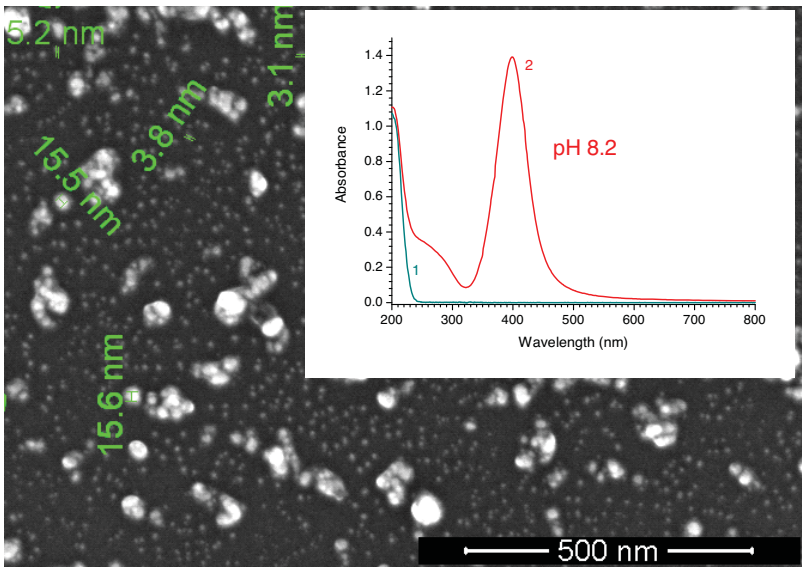


**FIG. 8:** Scanning electron microscopy image of silver nanoparticles extracted from the solution after 5 minutes of treatment with helium + 5% $H_2$ plasma with bipolar pulses. Inset: absorption spectra of the solution (0.1 mmol/L $AgNO_3$) before (1) and after (2) 5 minutes of plasma treatment.

SEM samples requires the NPs to be removed from the solution and dried, which may cause further aggregation of NPs in the increasingly concentrated solution; therefore the fraction of aggregates in Fig. 8 is probably overemphasized.

Additional information about the size of Ag NPs in freshly prepared colloids can be analyzed in situ using DLS. One should keep in mind the $d^6$ dependence of the DLS signal ($d$ is the effective hydrodynamic diameter of the scatterers), so the primary raw data overestimate the contribution of larger particles to the weighted distribution of the scattering intensity at the expense of smaller ones.[25] The size distribution of Ag NPs in the number-weighted mode is shown in Fig. 9 (Figs. 8 and 9 refer to the same batch).

Thus, 2 clearly distinguished fractions of NPs are observed; the majority of particles are very small (~2 nm), and the fraction of aggregates with a size of about 20 nm is insignificant. The presence of some amount of large particles as strong scatterers should generally not compromise the accuracy of DLS measurements.[26] The difference between the sizes of the NPs detected by SEM and DLS is not large. It can be concluded that only small Ag NPs (~2 nm) are responsible for the narrow plasmonic absorption peak in Fig. 7, and both the number of agglomerates and their contribution to absorption are negligible.

In addition to size, the stability of NPs in a solution is another important factor. Solutions of surfactant-free Ag NPs can be stored at room temperature for several months without any sign of agglomeration. The persistence of Ag NPs can be explained by zeta potential measurements. A value of −41 mV (for the same batch as in Fig. 8) indicates a negative net charge of Ag NPs at pH 8.2. This charge decreases over the course of titration with acid. However, the as-prepared colloid remains stable upon the addition of $HNO_3$ until the pH reaches a value of 4. An increase in the proton concentration can reduce the thickness of the electric double layer, neutralize the negatively charged metal–water interface, and destabilize NPs, so the formation of loose aggregates may occur. As several colloid chemistry studies suggest, the hydrophobic surfaces of different noble

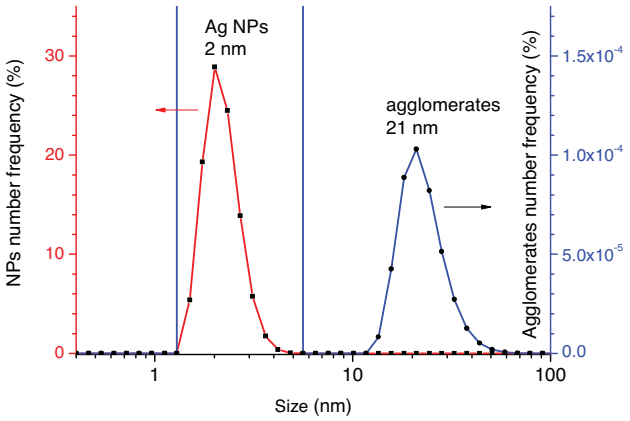


**FIG. 9:** Size distribution of silver (Ag) nanoparticles (NPs) (as weighted number density) in a solution after 5 minutes of treatment of 0.1 mmol/L AgNO3 with helium + 5% $H_2$ plasma with bipolar pulses. Distribution is measured using the dynamic light scattering technique.

metals accumulate a negative charge when dipped in pure water; this is explained by the surface adsorption of $OH^-$ ions.[4,27,28] Preferential orientation of the water molecules at the water–metal interface could provide a driving force for the migration and extra adsorption of $OH^-$ ions. As a result, the adsorbed $OH^-$ ions are also oriented with the hydrogen pointing away from the surface and toward the liquid.[29]

An electrostatic stabilization scheme is shown for Ag NPs using a possible analogy with gold NPs[4,30] (Fig. 10). Under acidic conditions, the surface of an Ag NP is slightly oxidized, with the formation of a partially protonated layer of $O^-$ species covalently bound to Ag atoms, resulting in a small negative surface charge. This charge is, however, not sufficient for effective stabilization. An increase in the pH of the solution can increase the negative surface charge through the additional adsorption of $OH^-$ ions on the free metal surface. Hence the remarkable stability of NPs is achieved, based on their electrostatic repulsion under slightly alkaline conditions. The dependence of the stability of Ag NPs on pH also shows that electrostatic stabilization is dominated by $OH^-$ ion adsorption, rather than by surface oxidation.

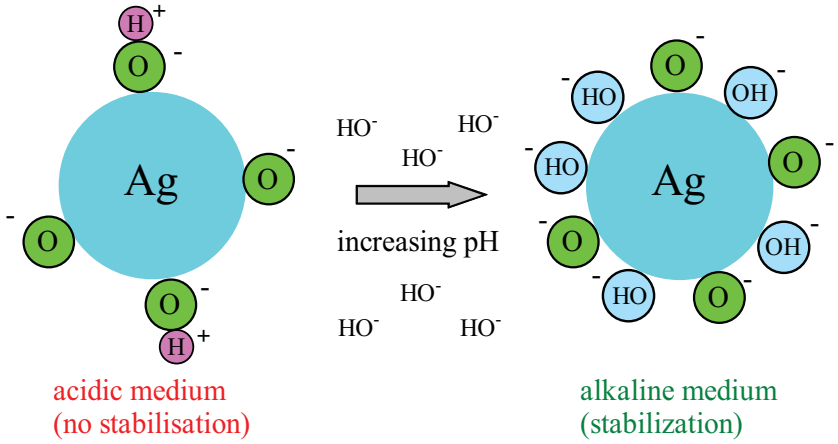


**FIG. 10:** The scheme of electrostatic stabilization mechanism for silver (Ag) nanoparticles in alkaline conditions.

At the high repetition rates of discharge (12 kHz), the particles formed during previous pulses do not have enough time to move away from the site where NPs and free Ag atoms are produced during a new pulse. As a result, the NPs accumulate near the interface, and their local concentration could be much higher than the average concentration in the bulk. When the local concentration becomes high enough, agglomeration can start. To prevent this process, electrostatic stabilization should occur very quickly close to the plasma–liquid interface. It could be favorable if the local density of $OH^-$ ions is high, as a result of the transformation of hydrated electrons into $OH^-$ ions.

Other than an atomic thin oxide layer and relatively weakly bound $OH^-$ ions, the surface of NPs produced with this technique can be considered "clean." This may constitute an important aspect, bearing in mind further functionalization or use in catalysis, biomedicine, or surface-enhanced Raman scattering (SERS) applications. Deposition of NPs on the surface of different support materials is necessary in most of these techniques. It was demonstrated that efficient adsorption of metal NPs (Ag, gold, Pt, iron) to surfaces of several support materials is best achieved with ligand-free NPs.[31]

## IV. CONCLUSION

The interactions between atmospheric-pressure He and $He/H_2$ pulsed-discharge plasmas and water solutions of $AgNO_3$, $HNO_3$, $KNO_3$ were investigated. The stable products resulting from plasma treatment are very sensitive to the chemical composition of the plasma and the polarity of the discharge. The treatment of water containing dissolved $N_2$ and $O_2$ with the pure He discharge with a negative polarity leads to the accumulation of both $HNO_3$ and $H_2O_2$. As expected, deaeration of the solution before plasma processing suppresses the formation of $HNO_3$. Contrary to the He discharge, plasma treatment of air-saturated water with the $He/H_2$ discharge with negative and, especially, bipolar pulses produces only traces of $HNO_3$ and no $H_2O_2$. The remarkable efficiency of the $He/H_2$ discharge with bipolar pulses for the nearly complete decomposition of $NO_3^-$ and slight alkalization of dilute $HNO_3$ and $KNO_3$ solutions was demonstrated. These reactions occur at the plasma–liquid interface with the participation of very short-lived species (hydrated electrons and ·H radicals). The difference in the efficiency of $NO_3^-$decomposition between bipolar (~90%) and negative-polarity (~10%) $He/H_2$ plasma processing was explained by the migration of $NO_3^-$ ions in electric field of the plasma–liquid interface.

An efficient method for the synthesis of small (~2 nm) Ag NPs through treatment of an $AgNO_3$ solution by $He/H_2$ discharge with bipolar pulses was developed. The solution of surfactant-free Ag NPs with a zeta potential of −41 mV at pH ~8 is very stable and does not show any agglomeration for months. Remarkably, the NPs are stable even when $HNO_3$ is added, achieving a pH as low as ~4. A shell of negatively charged $OH^-$ ions adsorbed on the surface of Ag NPs could be responsible for electrostatic stabilization in a slightly alkaline environment.

We conclude that the treatment of water solutions by $He/H_2$ discharge with bipolar pulses achieves the best results in the decomposition of $NO_3^-$ and slight alkalization of the solutions. This treatment should be considered as optimal for the synthesis of small, ligand-free, electrostatically stabilized Ag NPs with a narrow size distribution and remarkable stability in the form of a colloidal solution in water.

## ACKNOWLEDGMENTS

The authors thank M. Visnapuu for performing the dynamic light scattering measurements, K. Herodes and K. Kroon for analyzing the cations using ion liquid chromatogra-

phy, and K. Tammeveski for useful discussions. The authors are grateful to I. Renge for the critical reading of this article and for fruitful and valuable discussions.

This work was supported by the Estonian Nanotechnology Competence Centre, the European Regional Development Fund Centres of Excellence ("Mesosystems: Theory and Applications," TK114), and the European Cooperation in Science and Technology (COST) Action TD1208 ("Electrical Discharges with Liquids for Future Applications").

## REFERENCES

1. Belloni J, Mostafavi M, Remita H, Marignier J-L, Delcourt M-O. Radiation-induced synthesis of mono- and multi-metallic clusters and nanocolloids. New J Chem. 1998;22(11):1239–55.
2. Gutierrez M, Henglein A. Formation of colloidal silver by "push-pull" reduction of Ag+. J Phys Chem. 1993;97(44):11368–70.
3. Choi S-H, Lee S-H, Hwang Y-M, Lee K-P, Kang H-D. Interaction between the surface of the silver nanoparticles prepared by γ-irradiation and organic molecules containing thiol group. Radiat Phys Chem. 2003;67(3–4):517–21.
4. Rehbock C, Jakobi J, Gamrad L, van der Meer S, Tiedemann D, Taylor U, Kues W, Rath D, Barcikowski S. Current state of laser synthesis of metal and alloy nanoparticles as ligand-free reference materials for nano-toxicological assays. Beilstein J Nanotechnol. 2014;5(1):1523–41.
5. Koo IG, Lee MS, Shim JH, Ahn JH, Lee WM. Platinum nanoparticles prepared by a plasma-chemical reduction method. J Mater Chem. 2005;15(38):4125–8.
6. Richmonds C, Sankaran RM. Plasma-liquid electrochemistry: rapid synthesis of colloidal metal nanoparticles by microplasma reduction of aqueous cations. Appl Phys Lett. 2008;93(13):131501.
7. Richmonds C, Witzke M, Bartling B, Lee SW, Wainright J, Liu C-C, Sankaran RM. Electron-transfer reactions at the plasma-liquid interface. J Am Chem Soc. 2011;133(44):17582–5.
8. Patel J, Němcová L, Maguire P, Graham WG, Mariotti D. Synthesis of surfactant-free electrostatically stabilized gold nanoparticles by plasma-induced liquid chemistry. Nanotechnology. 2013;24(24):245604.
9. Lin L, Wang Q. Microplasma: a new generation of technology for functional nanomaterial synthesis. Plasma Chem Plasma Process. 2015;35(6):925–62.
10. Huang XZ, Zhong XX, Lu Y, Li YS, Rider a E, Furman SA, Ostrikov K. Plasmonic Ag nanoparticles via environment-benign atmospheric microplasma electrochemistry. Nanotechnology. 2013;24:095604.
11. Sander R. Compilation of Henry's law constants (version 4.0) for water as solvent. Atmos Chem Phys. 2015;15(8):4399–981.
12. Yonemori S, Ono R. Flux of OH and O radicals onto a surface by an atmospheric-pressure helium plasma jet measured by laser-induced fluorescence. J Phys D Appl Phys. 2014;47(12):125401.
13. Lukes P, Dolezalova E, Sisrova I, Clupek M. Aqueous-phase chemistry and bactericidal effects from an air discharge plasma in contact with water: evidence for the formation of peroxynitrite through a pseudo-second-order post-discharge reaction of H2O2 and HNO2. Plasma Sources Sci Technol. 2014;23(1):015019.
14. Norberg SA, Tian W, Johnsen E, Kushner MJ. Atmospheric pressure plasma jets interacting with liquid covered tissue: touching and not-touching the liquid. J Phys D Appl Phys. 2014;47(47):475203.
15. Le T, Tao S. Intrinsic UV absorption spectrometry observed with a liquid core waveguide as a sensor technique for monitoring ozone in water. Analyst. 2011;136(16):3335–42.
16. Oehmigen K, Winter J, Hähnel M, Wilke C, Brandenburg R, Weltmann K-D, von Woedtke T. Estimation of possible mechanisms of Escherichia coli inactivation by plasma treated sodium chloride solution. Plasma Process Polym. 2011;8(10):904–13.

17. Burlica R, Kirkpatrick MJ, Locke BR. Formation of reactive species in gliding arc discharges with liquid water. J Electrostat. 2006;64(1):35–43.
18. Long R, Zhou S, Wiley BJ, Xiong Y. Oxidative etching for controlled synthesis of metal nanocrystals: atomic addition and subtraction. Chem Soc Rev. 2014;43(17):6288–310.
19. Rumbach P, Bartels DM, Sankaran RM, Go DB. The solvation of electrons by an atmospheric-pressure plasma. Nat Commun. 2015;6:7248.
20. Buxton GV, Greenstock CL, Helman WP, Ross AB. Critical review of rate constants for reactions of hydrated electrons, hydrogen atoms and hydroxyl radicals (.OH/.O−) in aqueous solution. J Phys Chem Ref Data. 1988;17(2):513–886.
21. Witzke M, Rumbach P, Go DB, Sankaran RM. Evidence for the electrolysis of water by atmospheric-pressure plasmas formed at the surface of aqueous solutions. J Phys D Appl Phys. 2012;45(44): 442001.
22. Rumbach P, Griggs N, Sankaran RM, Go DB. Visualization of electrolytic reactions at a plasma-liquid interface. IEEE Trans Plasma Sci. 2014;42(10):2610–1.
23. Wilcoxon JP, Martin JE, Provencio P. Optical properties of gold and silver nanoclusters investigated by liquid chromatography. J Chem Phys. 2001;115(2):998–1008.
24. Farrag M, Thämer M, Tschurl M, Bürgi T, Heiz U. Preparation and spectroscopic properties of monolayer-protected silver nanoclusters. J Phys Chem C. 2012;116(14):8034–43.
25. Berne BJ, Pecora R. Dynamic light scattering: with applications to chemistry, biology, and physics. Mineola, NY: Dover Publications; 2000.
26. Filipe V, Hawe A, Jiskoot W. Critical evaluation of nanoparticle tracking analysis (NTA) by NanoSight for the measurement of nanoparticles and protein aggregates. Pharm Res. 2010;27(5):796–810.
27. Marinova KG, Alargova RG, Denkov ND, Velev OD, Petsev DN, Ivanov IB, Borwankar RP. Charging of oil–water interfaces due to spontaneous adsorption of hydroxyl ions. Langmuir. 1996;12(8): 2045–51.
28. Cataliotti RS, Aliotta F, Ponterio R. Silver nanoparticles behave as hydrophobic solutes towards the liquid water structure in the interaction shell. A Raman study in the O-H stretching region. Phys Chem Chem Phys. 2009;11(47):11258–63.
29. Zangi R, Engberts JB. Physisorption of hydroxide ions from aqueous solution to a hydrophobic surface. J Am Chem Soc. 2005;127(7):2272–6.
30. Rehbock C, Merk V, Gamrad L, Streubel R, Barcikowski S. Size control of laser-fabricated surfactant-free gold nanoparticles with highly diluted electrolytes and their subsequent bioconjugation. Phys Chem Chem Phys. 2013;15(9):3057–67.
31. Wagener P, Schwenke A, Barcikowski S. How citrate ligands affect nanoparticle adsorption to microparticle supports. Langmuir. 2012;28(14):6132–40